Bioconjugate Chemistry

Article

pubs.acs.org/bc

Fluorescently Labeled Cyclodextrin Derivatives as Exogenous Markers for Real-Time Transcutaneous Measurement of Renal Function

Jiaguo Huang,[†,⊥] Stefanie Weinfurter,[†,⊥] Pedro Caetano Pinto,[‡] Marc Pretze,[§] Bettina Kränzlin,[†] Johannes Pill,[†] Rodeghiero Federica,[∥] Rossana Perciaccante,[∥] Leopoldo Della Ciana,[∥] Rosalinde Masereeuw,[‡] and Norbert Gretz*[,†]

[†]Medical Research Center, Medical Faculty Mannheim, University of Heidelberg, 68167 Mannheim, Germany

[‡]Division of Pharmacology, Utrecht Institute for Pharmaceutical Sciences, Utrecht University, 3584 CG Utrecht, The Netherlands

[§]Molecular Imaging and Radiochemistry, Department of Clinical Radiology and Nuclear Medicine, Medical Faculty Mannheim, University of Heidelberg, 68167 Mannheim, Germany

[∥]Cyanagen S.r.l., 40138 Bologna, Italy

Supporting Information

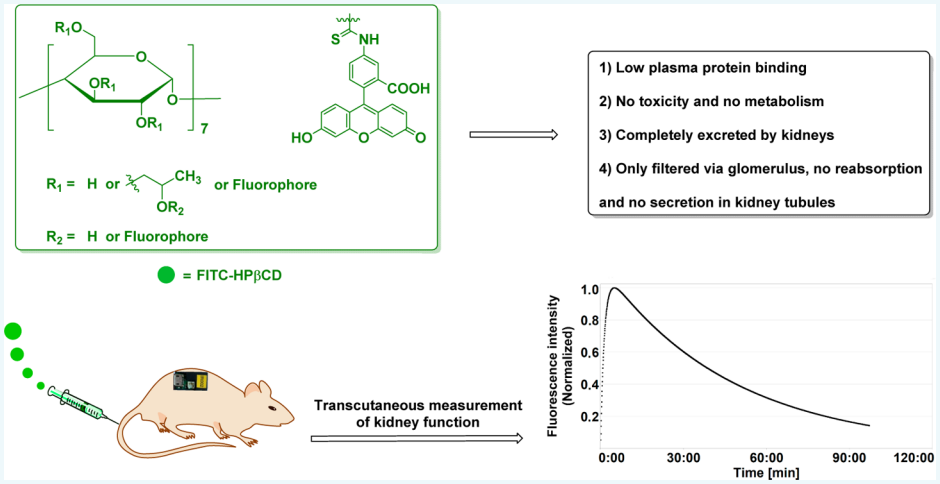

ABSTRACT: Evaluation of renal function is crucial for a number of clinical situations. Here, we reported a novel exogenous fluorescent marker (FITC−HPβCD) to real-time assess renal function by using a transcutaneous fluorescent detection technique. FITC−HPβCD was designed based on the principle of renal clearance of designed drugs. It displays favorable fluorescent properties, high hydrophilicity, low plasma protein binding, and high stability in porcine liver esterase as well as in plasma and nontoxicity. More importantly, FITC−HPβCD can be efficiently and rapidly filtered by glomerulus and completely excreted into urine without proximal tubular reabsorption or secretion in rat models. Additionally, the marker was well-tolerated, with nearly 100% urinary recovery of the given doses, and no metabolism were found. Relying on this novel kidney function marker and transcutaneous devices, we demonstrate a rapid, robust, and convenient approach for real-time assessing renal function without the need of time-consuming blood and urine sample preparation. Our work provides a promising tool for noninvasive real-time monitoring of renal function in vivo.

INTRODUCTION

Renal damage affects the ability of the kidney to remove xenobiotics and metabolic products from blood.[1,2] Accurate measurement of renal function is crucial for the detection and treatment of kidney failure.[3] Especially in the case of impaired kidney function, accurate assessment of renal function is essential for detecting renal failure in early stages of the disease, evaluating interventions and monitoring changes of function over time.[3,4] Glomerular filtration rate (GFR) is considered the best indicator for overall renal function.[5,6] GFR cannot be measured directly; the most common method of measuring GFR is based on the concept of clearance, the renal clearance of a substance can be defined as the volume of plasma from which substance is completely cleared per unit of time.[7,8]

Received: August 13, 2016
Revised: September 9, 2016
Published: September 9, 2016

DOI: 10.1021/acs.bioconjchem.6b00452
Bioconjugate Chem. 2016, 27, 2513−2526

Scheme 1. Structures of (a) Exogenous and (b) Endogenous [29] Renal Function Markers and (c) Novel Exogenous Markers Fluorescein−HPCDs, FITC−HPCDs, and XITC−HPCDs

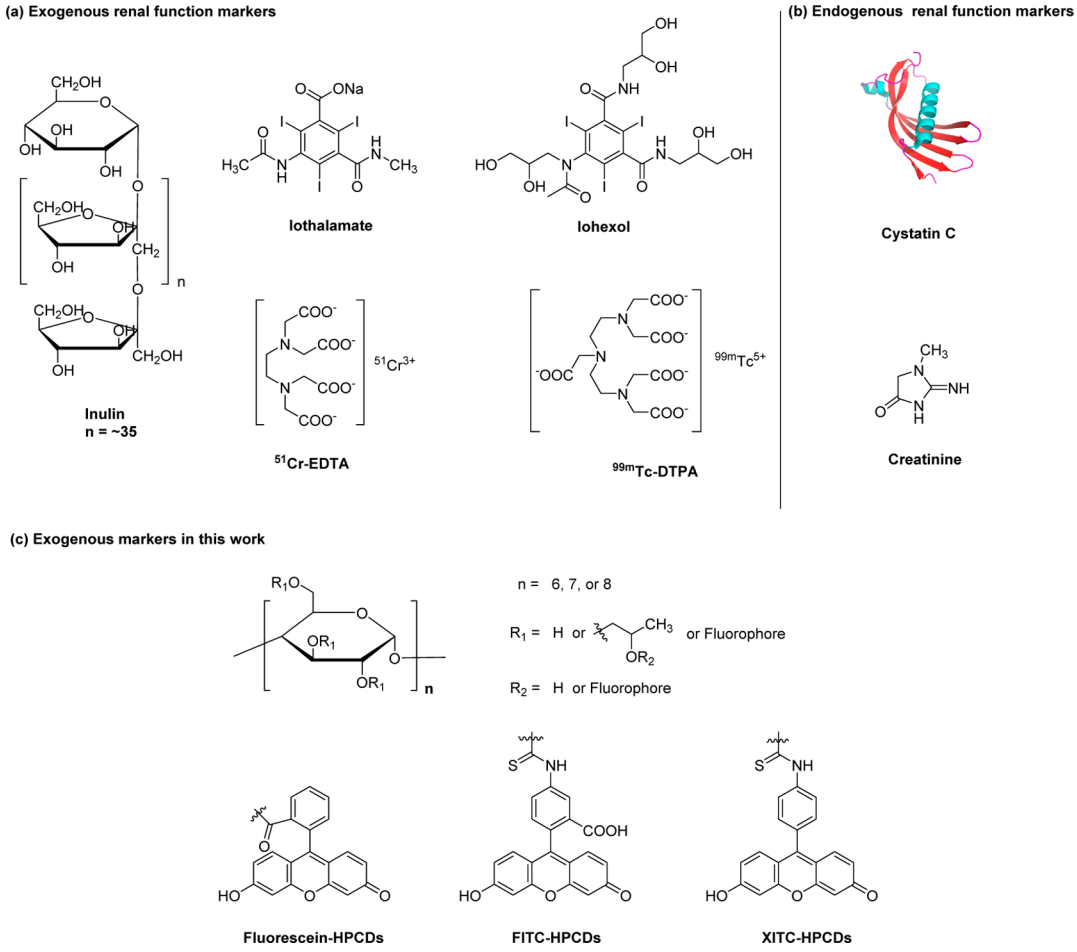

Endogenous markers, such as creatinine and cystatin C as well as several exogenous agents including inulin, ^{99m}Tc-DTPA, and iothalamate (Scheme 1 and Table S2), have been developed to determine GFR in the past several decades. Plasma creatinine concentration is commonly used to estimate GFR; however, creatinine is a product of the metabolism of creatine in muscles. Therefore, this parameter may be misleading because it is affected by age, gender, muscle mass, diet, and many other anthropometric variables.[9] Moreover, many studies revealed that creatinine is not only filtered by the glomerulus but also secreted by proximal tubule cells, leading to creatinine clearance exceeding GFR.[1,9,10] Furthermore, plasma clearance of exogenous agents including iothalamate and ^{99m}Tc-DTPA have been used to measure GFR. Those methods suffer from the complexity of ex vivo handling of blood and urine samples or disposal of radioactivity.[1] GFR can be determined by injecting inulin because inulin is neither reabsorbed nor being secreted by the proximal tubule after glomerular filtration, so its rate of excretion is directly proportional to the rate of filtration of water and solutes across the glomerular filter. Therefore, inulin is considered as the "gold standard" agent.[11] Nevertheless, it is difficult to handle due to poor water solubility and limited availability.[11] Also, determinations of the plasma and urinary clearance of exogenous renal markers are cumbersome, invasive, and very time-consuming due to the requirement of multiple blood and urine sampling and tedious sample analysis by HPLC.[1,12]

Many attempts had been made to overcome those limitations. Recently, fluorescent GFR markers have gained much attention. However, very few fluorescent compounds have been reported as true GFR markers so far. Only two kinds of fluorescent GFR markers have been reported from animal experiments. First, Dorshow et al. made great efforts by focusing on the development of fluorescent GFR markers based on two general approaches. One of the approaches involved enhancing the fluorescence of known or existing renal agents, which are intrinsically poor emitters, such as lanthanide-metal complexes. However, the results suggested that these complexes are excreted not only via glomerular filtration but also through tubular secretion, leading to a bias in GFR measurement.[13] The other approach was based on transforming highly fluorescent dyes into hydrophilic and anionic substances to force them to be excreted by kidneys. Although hydrophilic pyrazine-dicaboxylic acid derivatives were developed, the sophisticated synthesis routes made them difficult to produce and expensive.[14−16] Second, earlier, inulin has been engineered in its fluorescein isothiocyanate conjugated variant for a single-bolus injection method in conscious animals.[17,18] Its elimination kinetics is typically obtained by measuring the fluorescent values in plasma over a specific period time after the bolus injection. Despite the highly reproducible results provided that no longer required urine sampling, the repeated blood sampling makes the method stressful and still in an invasive manner; moreover, the necessity to heat and dialyze

DOI: 10.1021/acs.bioconjchem.6b00452
Bioconjugate Chem. 2016, 27, 2513−2526

Scheme 2. (a) Synthesis of Decarboxylated FITC and XITC and (b) Synthesis of Fluorescein−HPCDs, FITC−HPCDs, and XITC−HPCDs

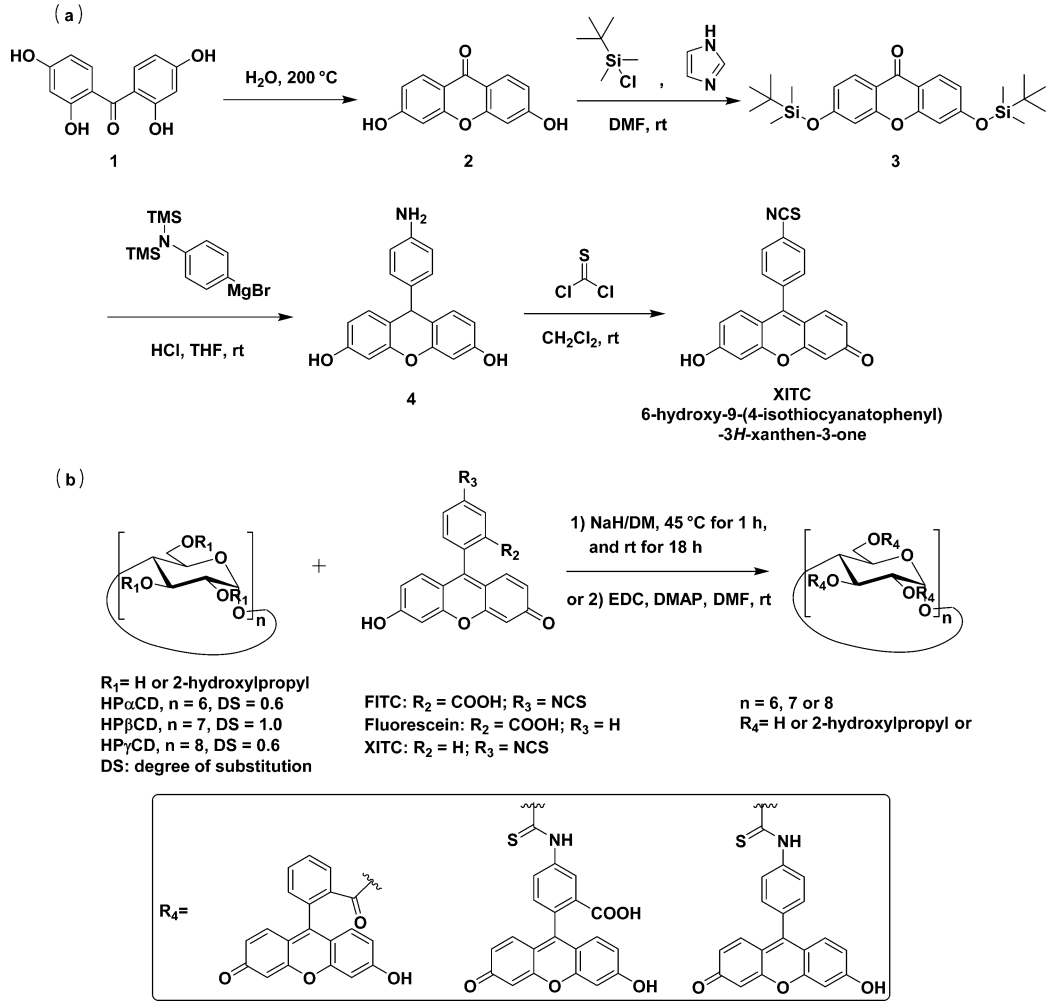

the FITC−inulin solution for removing residual unbound FITC makes the procedure cumbersome.[17,18] In keeping with these observations, it is urgent to overcome the poor solubility of FITC−inulin, as well as plasma sample collection and analysis. In our previous studies, we, on one hand, successfully developed FITC−sinistrin instead of FITC−inulin[19−21] due to its better water solubility and lack of need to dialyze before injection; on the other hand, we developed a noninvasive transcutaneous measurement for the elimination kinetics of fluorescent FITC−sinistrin marker based on a miniaturized electronic device attached to the skin.[22−28] The major advantage of this approach is their independence from blood and urine sampling and laboratory assays. Therefore, allowing renal function assessment in real-time and making the evaluation of rapid changes in renal function possible (for example, in acute renal failure). Importantly, more-precise results of the plasma clearance can be obtained via transcutaneous real-time measurement, which relies on a high number of data points rather than a limited number of data points from blood and urine sampling. Nevertheless, both inulin and sinistrin suffered from their inherent limitations, such as high cost, limited availability, sophisticated extraction, and purification from plants roots. Therefore, there is an unmet challenge to develop novel fluorescent GFR markers for noninvasive real-time assessing renal function.

Here, we report 2-hydroxylpropyl-cyclodextrins (HPCDs)-based fluorescent markers (Scheme 1c) for transcutaneous assessment of kidney function. FITC−HPCDs markers are judiciously designed by combining the basic principle of renally cleared drugs and the knowledge of a cyclodextrin-based drug delivery system. These markers can be easily synthesized and have favorable fluorescent properties, high hydrophilicity, low plasma protein binding (PPB), and high stability in porcine liver esterase as well as in plasma and nontoxicity. More significantly, FITC−HPβCD can be excreted efficiently and rapidly through kidneys into urine without reabsorption and secretion in kidney tubule. This is in agreement with a previous study that 99% administered cyclodextrin can be excreted to urine within 12 h.[30] High urinary recovery further demonstrates that it is completely renally cleared without metabolism in vivo. Due to these favorable properties, FITC−HPβCD has a high potential to be an exogenous marker for noninvasive real-time transcutaneous assessment of renal function.

RESULTS AND DISCUSSION

Design and Synthesis. An ideal exogenous fluorescent marker for transcutaneous assessment of GFR should meet certain requirements,[14] such as (1) excitation and emission wavelengths in the visible region or near-infrared range; (2) highly hydrophilicity and neutral or anionic charge; (3) very

DOI: 10.1021/acs.bioconjchem.6b00452
Bioconjugate Chem. 2016, 27, 2513−2526

Table 1. Photophysical Properties of Free Dyes and Their HPCD-Based Markers

entry	λ_{abs} (nm) PBS/plasma	λ_{em} (nm) PBS/plasma	stokes shift (nm)	ε (M^{-1} cm^{-1})	net charge (pH = 7.0)	MW [Da]	log D (pH = 7.4)	DOL[a]
FITC	494/496	520/523	26	70000	−1	389.38	−0.70	NA[b]
FITC- HPαCD	490/494	522/525	32	ND[c]	−1	1400−1800	−9.30	0.081
FITC- HPβCD	490/494	522/525	32	ND	−1	1700−2100	−10.70	0.080
FITC- HPγCD	490/494	522/525	32	ND	−1	2000−2400	−10.95	0.082
fluorescein	494/498	520/525	26	68000	−1	332.31	−1.30	NA
fluorescein - HPαCD	498/500	534/537	36	ND	0	1400−1750	−5.53	0.055
fluorescein - HPβCD	498/500	534/537	36	ND	0	1700−2050	−6.93	0.043
fluorescein - HPγCD	498/500	534/537	36	ND	0	2000−2350	−8.33	0.049
XITC	494/500	530/531	36	16800	0	345.04	3.06	NA
XITC- HPαCD	498/500	530/531	32	ND	0	1400−1760	−5.55	0.101
XITC- HPβCD	498/500	530/531	32	ND	0	1700−2060	−6.95	0.123
XITC- HPγCD	500/500	530/531	30	ND	0	2000−2360	−7.20	0.114

[a]DOL: degree of labeling. [b]NA: not applicable. [c]ND: not determined.

low or no PPB; (4) nontoxicity and no metabolism in vivo; (5) no reabsorption and no secretion in kidney tubules, filtrated only by the glomerulus; and (6) ease of production with low costs. It is necessary to take all of these characteristics into account for a rational GFR marker design. To meet these criteria, a series of fluorescent markers were designed that comprise the two key functional components: 2-hydroxylpropyl-CDs (HPCDs) and fluorophores. First, introducing HPCDs is attempted to increase water solubility, decrease PPB, and accelerate excretion for fluorescent markers. Among various native cyclodextrins (CDs) and CDs derivatives, 2-hydroxylpropyl-αCD, -βCD, and -γCD (abbreviated as HPαCD, HPβCD, and HPγCD in below) not only have better water solubility than their native CDs (Table S3) but are also more stable to resist the hydrolysis by α-amylases of either porcine or human origin.[31] γCD can be hydrolyzed relatively fast and extensively (80% in 24 h) by α-amylases.[31] However, the degradation rates of αCD, βCD, HPαCD, and HPβCD are limited and slow (only 2% in 24 h) by porcine pancreatic α-amylases.[31] The merits of no toxicity resulted in a FDA approval ten years ago.[32−34] Additionally, their narrow molecular weight distribution, low costs, and sufficient availability[32−35] make them an ideal backbone of GFR agents. Second, fluorescent dyes belonging to the xanthene family with appealing properties, such as physiological stability and safety profile, were employed for labeling HPCDs. Furthermore, we expanded our panel of xanthene fluorophores based on decarboxylated FITC, referred to as XITC (Scheme 2a), to study the different conjugation bonds and sites between fluorophore and HPCDs systematically. It is noticeable that anionic and neutral substances are preferentially cleared through the renal system;[14] therefore, rhodamine-based dyes were not chosen as fluorophores for labeling due to the positive charge of the aniline nitrogens or diethylaniline group. The three resulting markers possess different covalent conjugation bonds and net molecular charge, which are likely to show different pharmacokinetics and pharmacodynamics.

The general synthetic routes of FITC−HPCDs, fluorescein−HPCDs, and XITC−HPCDs are illustrated in Scheme 2. The synthesis of compound XITC was carried out following an efficient synthetic procedure[36−38] depicted in Scheme 2a. Bisphenolic precursor 2 can be easily accomplished under high temperature in special pressurized flasks. Based on a nucleophilic addition of Grignard derivative to a TBDMS-protected 3,6-dihydroxy-xanthenone and a subsequent dehydration with aqueous hydrochloric acid,[36,39] the corresponding amine product 4 was obtained. Treatment of this compound with an excess of thiophosgene under basic conditions yielded the isothiocyanate product XITC. The synthesis of three different markers is easily done in a one-step reaction (Scheme 2b).[40−42] All intermediates and markers were characterized by ^{1}H NMR, ^{13}C NMR, and low resolution-mass spectrometry (LR-MS).

Physicochemical Characteristics and Optical Properties. The spectroscopic and physicochemical properties are summarized in Table 1. All conjugated compounds showed absorption peaks in the wavelength range between 490 to 500 nm either in PBS or Sprague−Dawley (SD) rat plasma (Table 1 and Figures 1a and S2) by irradiation at 480 nm, all the markers displayed emission peaks around 520 to 530 nm, which is consistent with the spectra of their free dye. Therefore, the introduction of HPCDs on the fluorophore moiety did not cause a shift in the spectra. Notably, their spectrum is effectively matching with the configuration of the transcutaneous device, which is composed of two light-emitting diodes with excitation wavelength of 480 nm and a photodiode for emission wavelength detection of 520 nm. Despite XITC having a simple structure, it is a novel compound in the xanthene family. Compared to FITC, the removal of carboxylic acid group on the *meso* aryl ring for eliminating the negative charge did not result in change in absorbance and emission spectra. However, the extinction coefficient of XITC is clearly lower than that of FITC[43] and fluorescein[44] (Table 1). This result is consistent with previous studies showing that the removal of a carboxylic acid group on the *meso* aryl ring allows the benzene moiety a free rotation, leading to a reduction of the extinction coefficient as well as a fluorescent quantum yield.[39]

Investigations of matrix-assisted laser desorption−ionization (MALDI) mass spectrometry provided further evidence for fluorophore-functionalized HPCDs. In Figure 5b, the mass of FITC−HPβCD features five peaks on the right part of the spectrum at m/z = 1720.235, 1778.272, 1836.320, 1894.366, and 1952.403 Da, corresponding to the calculated mass of native HPβCD plus FITC, respectively. A distribution corresponding to the mass of unmodified native HPβCD is also observed at m/z = 1331.368, 1389.395, 1447.423,

DOI: 10.1021/acs.bioconjchem.6b00452
Bioconjugate Chem. 2016, 27, 2513−2526

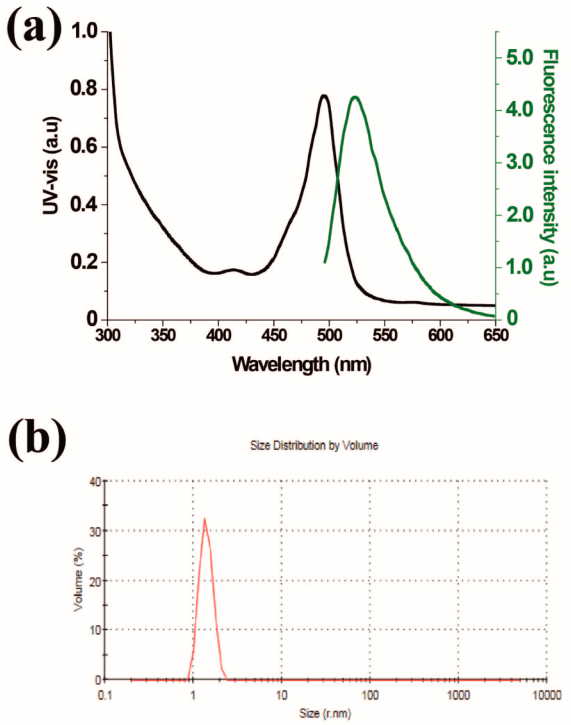

Figure 1. (a) Absorption and emission spectra of FITC−HPβCD in rat plasma. (b) The size of FITC−HPβCD was analyzed by DLS.

1505.459, and 1563.495 Da on the left part of the spectrum. The 2D (^{1}H−^{1}H NOESY) spectra of FITC−HPβCD and fluorescein−HPβCD were investigated as shown in Figure S23 and S24; the cross-peak in the NOESY spectrum of both FITC−HPβCD and fluorescein−HPβCD clearly demonstrates that the HPCD's interior protons gave the NOE correlations with the aromatic protons of xanthene moiety in either FITC or fluorescein. The protons of δ 6.7−7.1 ppm were assigned to the xanthene protons and exhibit cross-peaks with the HPCD protons (δ 3−4 ppm), suggesting that a partial fluorophore moiety is encapsulated into the cavity of HPβCD. Distribution coefficient calculations using the JChem plugin of ChemAxon indicated that all the markers had excellent hydrophilicity with the log *D* value at pH 7.4 below −5 and varied with different dyes conjugation and HPCDs (Table 1). The net charge of the compounds spans a range from 0 to −1, depending on the absence or functionalization of carboxylic acids. The degree of labeling (DOL)[45] is defined as the average number of dye molecules coupled to HPβCD; the DOL of all the markers were determined as shown in Table 1, and low DOL (<0.13) is the aim for preserving the properties of HPCDs. Although the DOL of XITC−HPCDs is higher than that of FITC−HPCDs and fluorescein−HPCDs, their absorbance and emission intensity is lower than FITC−HPCDs and fluorescein−HPCDs in the same concentration. This is ascribed to the low extinction coefficient and fluorescent quantum yield of XITC, suggesting that a higher dose of XITC−HPCDs might be needed in animal experiments.

Aggregation Analysis. It has been postulated that macromolecules over 70 kDa or big nanoparticles cannot pass through the glomerular filter into urine under normal conditions.[46] In addition, the possible presence of βCD aggregates in a critical aggregation concentration 3 mM βCD was determined by dynamic light scattering (DLS) in previous studies.[47−50] Therefore, DLS measurements of FITC−sinistrin, FITC−HPCDs, and fluorescein−HPCDs at 3 mM concentrations in aqueous solutions were performed to further investigate their aggregation phenomenon (Figures 1b and S5 and Table S8). The hydrodynamic diameter of FITC-sinistrin is roughly 21.9 nm, which is likely due to a molecular weight range of 2000 to 6000 Da. Mean diameters in size distribution by volume ranging from 0.6 to 3 nm for FITC−HPCDs and fluorescein−HPCDs were observed. On the basis of these results and the actual value of the outer diameter (1.46, 1.54, and 1.75 nm) and the height (0.79 nm) of αCD, βCD, and γCD, respectively (Table S3), we conclude that each of the markers is in its monomeric unit or containing two or three units at most.

Plasma Protein Binding. Of particular significance for the suitability of fluorescent markers as GRF markers is the knowledge of their interaction with plasma proteins because binding to proteins influences the resulting pharmacokinetics, including biodistribution and excretion.[51] PPB studies were carried out for all of the markers using the assay described before.[52−54] Each of the markers was incubated with rat plasma at 37 °C for 1 h. The incubated markers were separated from nonabsorbed protein by equilibrium dialysis of PBS against dye-protein stock solution using a two-chamber dialysis setup. After 24 h, the concentrations of markers in both PBS and plasma were determined. As shown in Tables 2 and Table S9−S17, all of the markers exhibited very low PPB (<10%), comparable to or even lower (i.e., better) than some of the "gold standard" renal markers such as iothalamate, ^{51}Cr-EDTA, and ^{99m}Tc-DTPA (Table S2). Furthermore, the free fluorophores adsorb to a larger amount of protein than HPCDs-based markers; for example, fluorescein exhibits 93.1% PPB,[55] thereby reflecting a greater tendency for proteins to bind to hydrophobic compound. In fact, most oral drugs have a lipophilic

Table 2. PPB, Urinary Recovery, and Half-Life with or without Probenecid Treatment

substance	PPB [%]	urinary recovery [%]	$T_{1/2}$ without probenecid [min]	$T_{1/2}$ with probenecid [min][b]	changes in half-life [%][a]
FITC−HPαCD	7.1	99.1 ± 2.6 (3)	38.0 ± 4.7 (6)[c]	32.2 ± 5.8 (6)	−15.3
FITC−HPβCD	2.3	103.4 ± 4.1 (3)	24.1 ± 3.2 (6)	23.6 ± 6.6 (6)	−2.1
FITC−HPγCD	2.8	100 ± 6.7 (3)	20.2 ± 3.2 (6)	18.1 ± 2.7 (9)	−10.9
fluorescein−HPαCD	0	57.7 ± 2.1 (3)	7.8 ± 4.3 (6)	13.3 ± 6.6 (6)	+70.5
fluorescein−HPβCD	0	52.2 ± 8.5 (3)	7.3 ± 2.8 (7)	9.6 ± 3.7 (7)	+31.5
fluorescein−HPγCD	2.4	44.3 ± 3.1 (3)	6.3 ± 1.3 (7)	9.4 ± 2.5 (7)	+49.2
XITC−HPαCD	9.5	ND[d]	ND	ND	ND
XITC−HPβCD	7.7	103.2 ± 5.4 (3)	31.3 ± 7.0 (3)	32.2 ± 4.8 (3)	+2.9
XITC−HPγCD	9.6	ND	ND	ND	ND

[a]Changes in half-life: $[T_{1/2\ \text{probenecid}} - T_{1/2\ \text{without probenecid}}]/[T_{1/2\ \text{Probenecid}}]$. [b]$T_{1/2}$: clearance half-life. [c](n): number of rats. [d]ND: not determined.

DOI: 10.1021/acs.bioconjchem.6b00452
Bioconjugate Chem. 2016, 27, 2513−2526

physicochemical property, which is associated with higher PPB and hepatic clearance; on the contrary, renally cleared drugs are hydrophilic and usually have a low PPB.[56] In this study, the extremely low PPB of HPCD-based markers was attributed to the introduction of hydrophilic HPCDs on those hydrophobic fluorophores structures, which increases their hydrophilicity and minimizes nonspecific interactions with serum proteins.

Stability Studies in Porcine Liver Esterase and Plasma. To determine the stability of conjugation bonds between HPCDs and fluorophore, we coincubated HPβCD-based markers with porcine liver esterase (PLE) for 24 h and then analyzed their stability with HPLC. No degradation was observed for all of HPβCD-based markers (Figure S6), as indicated by no appearance of free fluorophore peak in HPLC chromatographs in comparison with three control measurements, including PLE, free fluorophore, and the corresponding marker, respectively. The ester bond of fluorescein−HPβCD in PLE is stable, which may be attributed to the effect of steric hindrance.[57] To gain further insight into the stability of these markers in plasma, we coincubated all the HPβCD-based markers with plasma. Similarly, no degradation was found after 24 h of incubation with rat plasma (Figure S7). The results revealed that HPβCD-based markers are stable in both PLE condition and plasma in vitro.

Cell Viability Evaluated by MTT Assay. The cytotoxicity of FITC−HPβCD and fluorescein−HPCDs was evaluated by using 3-(4,5-dimethyl-2-thiazoly)-2,5-diphenyltetrazolium bromide (MTT) assay, in conditionally immortalized human renal proximal tubule cell line (ciPTEC).[58] The results (Figures 2 and S8) show that FITC−HPβCD and fluorescein−HPCDs did not affect the viability of both of the two cell types tested (organic anion transporters 1 or 3 (OAT1 or OAT3) transfected), as compared to the results from the control group with untreated cells, suggesting that these markers have

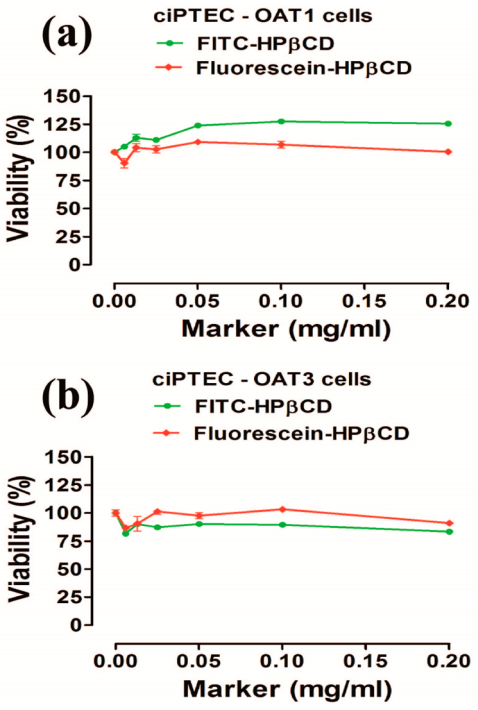

Figure 2. Cell viability of (a) ciPTEC-OAT1 and (b) ciPTEC-OAT3 cells incubated with FITC−HPβCD and fluorescein−HPβCD in MTT assays.

no significant cytotoxic effect in representative human renal cell lines. These nontoxicity results are also in agreement with previous reports using βCD derivatives on other cell lines.[59]

Transcutaneous Measurement of Renal Function in Rat Models. Encouraged by those excellent properties in vitro, we proceeded to investigate whether these HPCDs-based markers can be excreted by kidneys in rats by using noninvasive transcutaneous measurements. The principles and methods of the transcutaneous technique are described in the Experimental section and shown in Figure 3a−c. Fluorescence elimination curves and kinetic parameters of all the markers can be found in Figures 3 and S9 and Table 2. Take FITC−HPβCD as an example (Figure 3d); the clearance curves of FITC−HPβCD returned to background within 2 h after intravenous injection, suggesting that it was excreted completely in this period and has a clearance half-life of 24.1 ± 3.2 min (Table 2). Furthermore, to determine whether FITC−HPβCD can be reabsorbed or secreted in addition to glomerular filtration in kidneys, probenecid, an inhibitor of organic anion transporter (OAT) proteins in kidney tubules,[60,61] was administered to block a tubular reabsorption and secretion pathway, and then fluorescence elimination curves were also measured transcutaneously for the same rats. The fluorescent signals descended to baseline and it has a similar clearance half-life (23.6 ± 6.6 min) in comparison to results without probenecid treatment (Figure 3e and Table 2). The clearance half-life of FITC−HPCDs either in the absence or the presence of probeneicd follows the order of FITC−HPαCD > FITC−HPβCD > FITC−HPγCD, supporting the idea that the elimination goes faster with increased size of HPCDs. Similar phenomena were observed for fluorescein−HPCDs (fluorescein−HPαCD > fluorescein−HPβCD > fluorescein−HPγCD). The clearance half-life of the tested markers also varied with the fluorophore scaffold used; for example, XITC−HPβCD > FITC−HPβCD > fluorescein−HPβCD. Either with or without probenecid treatment, fluorescein−HPCDs were excreted extremely fast (Figure 3f,g) and have a shorter clearance half-life than FITC−HPCDs or XITC−HPβCD. In FITC−HPCDs, FITC−HPαCD and FITC−HPγCD have a slight tubular reabsorption because shorter clearance half-lives were observed in the presence of probenecid (Figure 4a). In contrast, fluorescein−HPCDs showed a significant higher half-life with probenecid treatment, which indicates tubular secretion in kidneys. Surprisingly, a negligible difference in half-life between the absence and presence of probenecid treatment for FITC−HPβCD and XITC−HPβCD was observed (Figure 4a), suggesting that FITC−HPβCD and XITC−HPβCD exhibit no tubular reabsorption or secretion and are cleared by glomerular filtration solely. Bland−Altman plots for transcutaneous measurement in the presence and absence probenecid treatment are depicted in Figure S10.

Urinary Recovery and Metabolism Studies. A mandatory prerequisite for an ideal renal function marker is to recover completely in urine and have no metabolism in vivo; therefore, we conducted recoveries of the injected doses using in vivo experiments with metabolic cages. Each marker was injected intravenously into rats. As shown in Figures 4 and S11 and Table S18, high urinary recoveries for FITC−HPαCD, FITC−HPβCD, and FITC−HPγCD of 99.1 ± 2.6%, 103.4 ± 4.1%, and 100 ± 6.7%, respectively, were observed. Considering that a low extinction coefficient of XITC and a higher dose of XITC−HPCDs might be needed in rats, XITC−HPβCD was chosen only for this trial. A similar tendency of urinary recovery

DOI: 10.1021/acs.bioconjchem.6b00452
Bioconjugate Chem. 2016, 27, 2513−2526

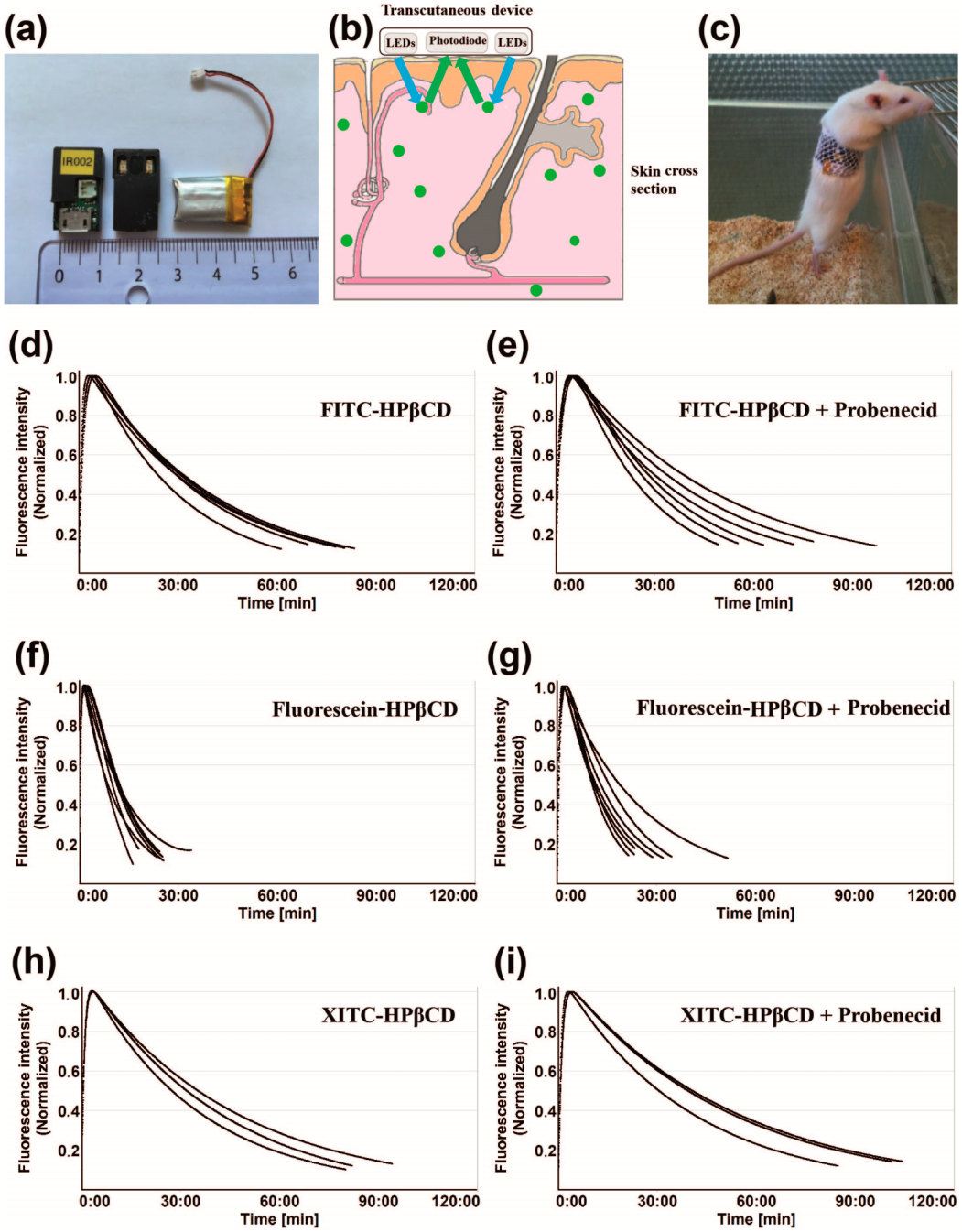

Figure 3. (a) Miniaturized transcutaneous devices and a battery used for the transcutaneous measurement of kidney function. (b) Fluorescent markers diffused from the vascular space to the interstitium after intravenous administration and its excretion was determined using a miniaturized electronic transcutaneous device. (c) A conscious SD rat is under transcutaneous measurement with an attached device. Elimination curves of FITC−HPβCD ((d,e); n = 6), fluorescein−HPβCD ((f,g); n = 7), and XITC−HPβCD ((h,i); n = 3) by transcutaneous measurements in SD rats models in the absence and presence of probenecid treatment.

(103.2 ± 5.4%; Figure 4d and Table S20) was also determined in the case of XITC−HPβCD. Indeed, urinary recovery of the given dose was almost completed at 6 to 9 h post-injection for FITC−HPβCD and FITC−HPγCD, which is in agreement with their short clearance half-life. These high urinary excretion rates indicated all the injected FITC−HPCDs and XITC−HPβCD are excreted into urine. However, only 40 to 60% of the injected doses were recovered for fluorescein−HPCDs (Figures 4c and S12 and Table S19). These results suggested that fluorescein−HPCDs are not completely excreted through the kidneys but also via other routes, including metabolism by enzymes in vivo.[62] The excretion profiles of fluorescein−HPCDs are consistent with their extremely short clearance half-life. Although fluorescein−HPCDs are stable under coincubation with PLE in vitro, the aromatic carboxylic acid ester on fluorescein−HPCDs is prone to hydrolysis in a complex environment in vivo.

Metabolism Studies. To evaluate whether these markers can be metabolized in vivo, urine samples were collected and investigated by HPLC. The HPLC results (Figure S14) indicate that metabolites were not formed. To better understand these results, we carried out an additional experiment by MALDI-

DOI: 10.1021/acs.bioconjchem.6b00452
Bioconjugate Chem. 2016, 27, 2513−2526

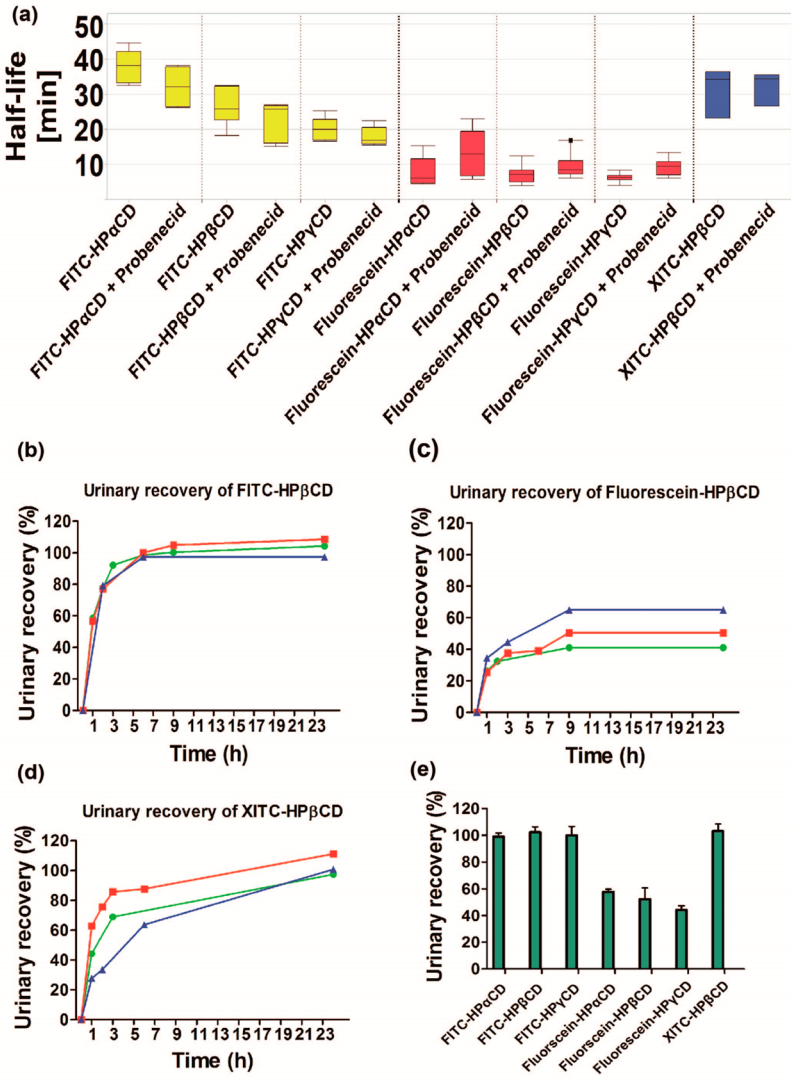

Figure 4. (a) Clearance half-life for each marker in the presence and absence of probenecid in rat models. (b) Urinary recovery for each marker in SD rats (n = 3) after 24 h. Urinary recovery-time curves of FITC−HPβCD (c), fluorescentin−HPβCD (d), and XITC−HPβCD (e) in SD rats (n = 3) over a period of 24 h.

time-of-flight (MALDI-TOF) analysis to confirm these markers in urine samples. The obtained MALDI-TOF data demonstrated that the mass distribution of FITC−HPβCD recovered from urine sample is the same as that of before injection (Figures 5c and S14). Therefore, we concluded that four substances, including FITC−HPαCD, FITC−HPβCD, FITC−HPγCD, and XITC−HPβCD, have high urinary recoveries of nearly 100% of the injected doses and do not undergo metabolism in vivo. However, FITC−HPαCD and FITC−HPγCD are reabsorbed slightly in kidney tubule and XITC suffers from undesirable optical properties, thus a higher dose of XITC−HPCDs might be required for in vivo studies. It should be emphasized that neither premature deaths nor adverse clinical signs in behaviors by measurement of body weight and food consumption of rats were observed during the whole experiments. Taken together, relying on the attractive features of FITC−HPβCD in vivo, including the complete and rapid excretion through kidneys into urine, exclusive filtration via glomerulus, and no reabsorption and secretion in kidney proximal tubules, it is considered as a promising novel exogenous fluorescent GFR marker. In contrast, FITC−HPαCD and FITC−HPγCD have a potential to determine the capacity of reabsorption function in kidney tubules.

CONCLUSIONS

To summarize, by considering the basic principle of renally cleared drug design and the knowledge of CD-based drug delivery system, we developed a type of novel fluorescent markers based on fluorophore-labeled HPCDs. Through a rational screening approach, FITC−HPβCD is considered the most-promising exogenous marker for transcutaneous GFR measurements. This marker can be easily synthesized and exhibits desirable fluorescence properties. In in vitro experiments, low plasma protein binding and good stability in plasma and esterase as well as no cytotoxicity were found. In rat models, a high urinary recovery of the given doses and no metabolism in vivo were observed. Noninvasive real-time monitoring of bolus clearance was determined in combination with a miniaturized electronic device for the transcutaneous fluorescence intensity detection in conscious rats. The results show no significant differences in clearance half-life of the markers in the absence and presence of probenecid treatment,

DOI: 10.1021/acs.bioconjchem.6b00452
Bioconjugate Chem. 2016, 27, 2513−2526

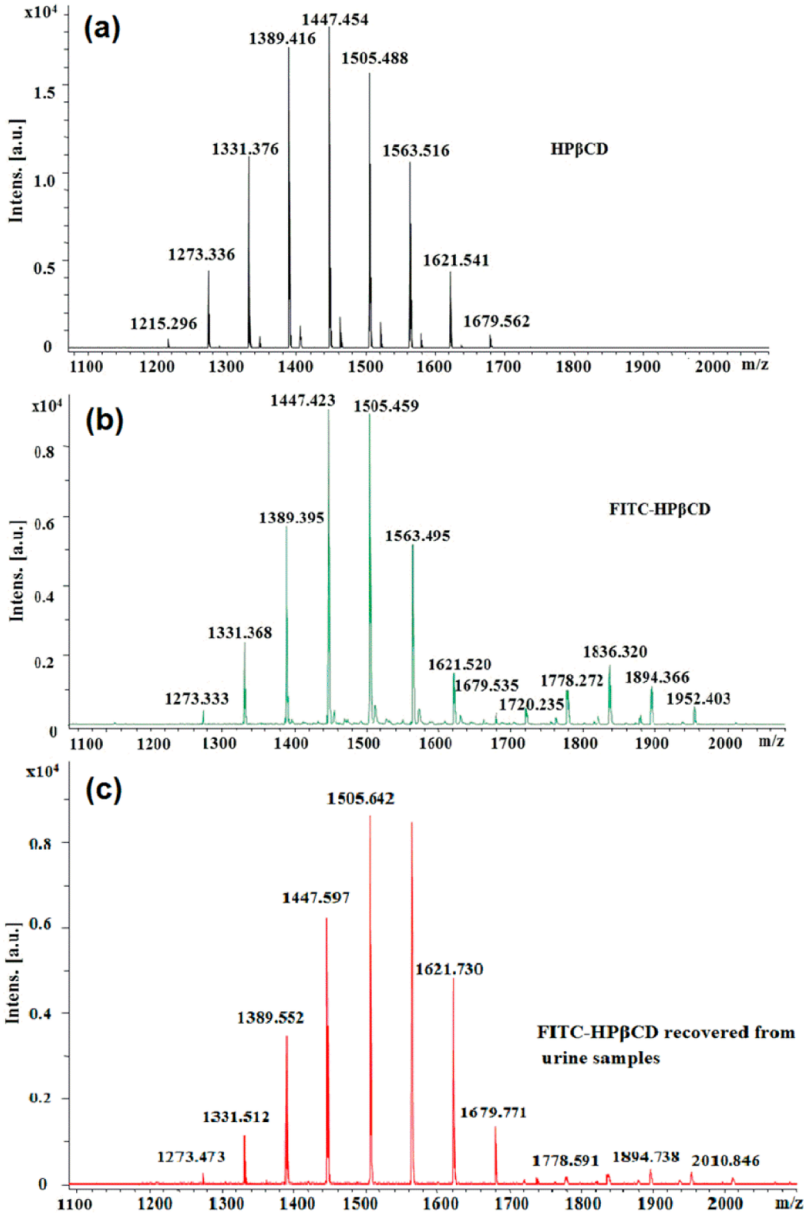

Figure 5. MALDI spectrum of (a) HPβCD, (b) FITC−HPβCD, and (c) FITC−HPβCD recovered from urine samples in SD rats.

so neither reabsorption nor secretion happened in kidney proximal tubule, demonstrating that it is filtrated by glomerulus only. To the best of our knowledge, this is the first use of cyclodextrin derivatives as a backbone for developing a novel GFR marker. Our platform of novel fluorescent markers combined with transcutaneous fluorescent detection technique enables a rapid, robust, and convenient monitoring of renal function without the need of time-consuming blood and urine sample preparation. Therefore, in the future, this method allows the assessment of renal function in real-time and the evaluation of rapid changes in renal function (for example, in acute renal failure). Formal preclinical development studies are in progress. Finally, we noted that the development of near-infrared transcutaneous devices and markers for deeper penetration depth will be an improvement for assessing kidney function.

EXPERIMENTAL SECTION

Materials. Reagents including fluorescent dyes (European Pharmacopoeia grade), anhydrous solvents (purity ≥99.9%), and deuterated solvents (99.96 atom % D, contains 0.03% (v/v) TMS) were purchased from Sigma-Aldrich or Carl Roth. All other solvents were used as supplied (HPLC-grade) without prior purification. Silica gel (Silicycle, 230−400 mesh) was used for column chromatography. The compounds 2-hydroxylpropyl-αCD, -βCD, and -γCD have degrees of substitution (DS) of 0.6, 1.0, and 0.6, respectively, and average molecular weights of 1180, 1540, and 1580 Da, respectively. The catalog numbers of 2-hydroxylpropyl-αCD, -βCD, and -γCD from Sigma-Aldrich are 390690-25G, 389145-25G, and 390704-25G, respectively. NMR spectra were recorded on a Bruker 300 MHz NMR instrument. Chemical shifts are reported in ppm relative to residual protic solvent resonances. Mestre Nova LITE v5.2.5-4119 software (Mestrelab Research S.L.) was used to analyze the NMR spectra. MALDI-TOF analyses were collected on a Bruker microflex instrument. UV−vis and fluorescence spectra were acquired using a microplate reader (Tecan Infinite M200) and an Eppendorf biospectrometer kinetic device using quartz cuvettes (1 cm path length). HPLC analysis and separations

DOI: 10.1021/acs.bioconjchem.6b00452
Bioconjugate Chem. 2016, 27, 2513−2526

were carried out on a Thermo Scientific Ultimate 3000 liquid chromatograph using Ascentis C18 columns. The pH of samples solution was tested by Mettler Toledo FiveEasy FE20pH bench meter. Dynamic light scattering studies were conducted using a Malvern Zetasizer Nano S90 equipment. IUPAC names of all compounds are provided and were determined using CS ChemBioDraw Ultra 12.0. The transcutaneous devices are available from Mannheim Pharma & Diagnostics, Mannheim, Germany.

Synthesis. *Synthesis of Compound 2.* A suspension of 2,2′,4,4′-tetrahydroxybenzophenone (compound 1, 2.46 g, 10 mmol) in 16 mL of H_2O was stirred and heated to 200 °C for 48 h. This reaction was accomplished in special pressure flask. The mixture was cooled to 60 °C, and then it was poured into 60 °C hot water and kept stirring 20 min. The yellow residue was filtered and extensively washed by 60 °C hot water until no start material was left over (monitored by TLC, EtOAc−nHex, 1/1). 3,6-dihydroxyxanthen-9-one (compound 2, 1.74 g) was obtained in a 76.3% yield. TLC (silica gel, EtOAc−nHex, 2/1) R_f = 0.28, ^{1}H NMR (300 MHz, DMSO-d_6, δ, ppm): 10.84 (s, 2H), 7.97 (d, J = 8.7 Hz, 2H), 6.84 (m, 4H). ^{13}C NMR (75 MHz, DMSO-d_6, δ, ppm): 173.87, 163.32, 157.43, 127.72, 113.96, 113.61, 102.05. LRMS (m/z): calcd, 228.05; found, 228.13.

Synthesis of Compound 3. To a solution of 3,6-dihydroxyxanthen-9-one (compound 2, 1.70 g, 7.45 mmol) and *tert*-butylchlorodimethyl silane (TBDMS-Cl, 6.90 g, 45.78 mmol) in DMF (30 mL), imidazole (5.20 g, 76.30 mmol) was added. The mixture was stirred at room temperature 12 h. The reaction was diluted by toluene (75 mL) and then extensively washed and extracted by water. The product was recrystallized from ethanol to receive the diprotected product (compound 3, 3.12 g) with a yield of 91%. TLC (silica gel, EtOAc−nHex, 2/1) R_f = 0.9, ^{1}H NMR (300 MHz, DMSO-d_6, δ, ppm): 7.94 (d, J = 9.1 Hz, 2H), 6.80 (m, 4H), 1.23 (s, 18H), 0.84 (s, 12H). LRMS (m/z): calcd, 456.22; found, 456.91. The characterization data are comparable with the previous reports.[38]

Synthesis of Compound 4. To a solution of xanthone diTBDMS ether (compound 3, 3.10 g, 6.78 mmol) in anhydrous THF was added phenylmagnesium bromide derivative (25 mL, 0.50 mol/mL in THF). This mixture was stirred under gas N_2 protection for 4 h. The reaction was quenched by adding 10 mL of 2 N HCl (aq) and stirred for 30 min, and then 5 mL of NaOH (3 mol/mL) was added dropwise to raise the pH of the mixture to 7.5 in an ice bath. The resulting yellow precipitate was filtrated, washed with a small volume of distilled THF, and dried in vacuum to yield a product (compound 4, 1.81 g, yield 87.6%). Further purification by silica gel column chromatography was done if required. LRMS (m/z): calcd, 303.09; found, 303.25.

Synthesis of Compound XITC. Thiophosgene (6 mL, 78 mmol) was dissolved in anhydrous CH_2Cl_2 (10 mL).This mixture was chilled to 0 °C in an ice bath. Product amine (compound 4, 1.80 g) was dissolved in anhydrous CH_2Cl_2 and added slowly in sequence. This mixture was allowed to warm to room temperature over 3 h. The mixture was concentrated under reduced vacuum and extensively washed by acetone to obtain 9-(4-isothiocyanatophenyl)-9H-xanthene-3,6-diol (compound XITC). TLC (silica gel, MeOH−EtOAc, 1/9) R_f = 0.5, ^{1}H NMR (300 MHz, DMSO-d_6, δ, ppm): 8.13 (d, J = 9, 1H), 7.71 (d, J = 9, 1H), 7.63 (s, 2H), 7.48 (m, 4H), 7.02 (d, J = 9, 2H). LRMS (m/z): calcd, 345.05.22; found, 345.57.

General Procedures for the Synthesis of FITC−HPαCD, FITC−HPβCD, and FITC−HPγCD. To a solution of (2-hydroxypropyl)-α-cyclodextrin (HPαCD, 800 mg) in DMF (8 mL), NaH (400 mg, 10 mmol, 60% suspension) was added slowly and stirred at room temperature. The reaction was stirred at 45 °C for 30 min. Afterward, FITC (100 mg, 0.26 mmol) was added, and the mixture was stirred at 45 °C for another 30 min and then kept at room temperature in the dark for 18 h. The red solution was cooled in an ice bath; saturated NH_4Cl solution was added then to adjust pH to near 10. Then, 5% acetic acid was added drop-wise to obtain a pH of 7.5. The solvent was concentrated under reduced pressure in a rotary evaporator (bath temperature 45 °C). The crude product was washed by acetone two times (300 mL each time) and filtered; the orange remains were purified by gel silica chromatographic column with gradient eluent (EtOAc, MeOH−EtOAc (1/2) and MeOH−H_2O (8/2)). The weight amount of silica gel per gram of crude products is 210 g. The eluent was concentrated under vacuum. For the transfer of this into a more-handleable form, the material is dissolved in 100 mL of H_2O at room tempertaure, filtered, and freeze-dried to yield a yellow solid FITC−HPαCD. According to the same procedure of FITC−HPαCD, FITC−HPβCD, and FITC−HPγCD were obtained. ^{1}H NMR (in D_2O), ^{13}C NMR (in D_2O), and mass spectrometry data are available in the Supporting Information.

General Procedures for the Synthesis of Fluorescein−HPαCD, Fluorescein−HPβCD, and Fluorescein−HPγCD. To a solution of (2-hydroxypropyl)-α-cyclodextrin (HPαCD, 2.0 g) and fluorescein (300 mg, 0.90 mmol) in DMF (10 mL), EDC (300 mg, 1.56 mmol) and DMAP (27 mg, 0.22 mmol) were added. The reaction was stirred without light at room temperature for 18 h. The resulting solution was concentrated under reduced pressure. The residue was purified by a gel silica chromatographic column with gradient eluent (EtOAc, MeOH−EtOAc (1/2), and MeOH−H_2O (8/2)). The weight amount of silica gel per gram of crude products is 210 g. The eluent was collected and concentrated under vacuum. This product was dissolved in water and freeze-dried to yield a red solid fluorescein−HPαCD. According to the same procedure as fluorescein−HPαCD, fluorescein−HPβCD and fluorescein−HPγCD were obtained. ^{1}H NMR (in D_2O), ^{13}C NMR (in D_2O), and mass spectrometry data are available in the Supporting Information.

General Procedures for the Synthesis of XITC−HPαCD, XITC−HPβCD, and XITC−HPγCD. To a solution of (2-hydroxypropyl)-α-cyclodextrin (HPαCD, 1.0 g) in DMF (8 mL), NaH (500 mg, 12.5 mmol, 60% suspension) was added slowly and stirred at room temperature. The reaction was stirred at 45 °C for 30 min. Afterward, XITC (100 mg, 0.29 mmol) was added, and the mixture was stirred at 45 °C for another 30 min and then kept at room temperature in the dark for 18 h. The red solution was cooled in an ice bath, and saturated NH_4Cl solution was added to adjust pH to near 10. Then, 5% acetic acid was added dropwise to obtain a pH of 7.5. The solvent was concentrated under reduced pressure in a rotary evaporator (bath temperature 45 °C). The crude product was washed by acetone two times (300 mL each time) and filtered; the orange remains were purified by a gel silica chromatographic column with gradient eluent (EtOAc, MeOH−EtOAc (1/2) and MeOH−H_2O (8/2)). The weight amount of silica gel per gram of crude products is 210 g. The eluent was concentrated under vacuum. To transfer this into a more-handleable form, the material is dissolved in 100 mL of

DOI: 10.1021/acs.bioconjchem.6b00452
Bioconjugate Chem. 2016, 27, 2513−2526

H_2O at room temperature, filtered, and freeze-dried to yield a yellow solid XITC−HPαCD. According to the same procedure of XITC−HPαCD, XITC−HPβCD, and XITC−HPγCD were obtained. ^{1}H NMR (in D_2O), ^{13}C NMR (in D_2O), and mass spectrometry data are available in the Supporting Information.

Optical Properties Characterization. Stock solutions of all of the compounds were prepared and stored at −20 °C. All the spectroscopic measurements were conducted in phosphate buffered saline (PBS), mixed with rat plasma, or both for the intended use. UV−vis and fluorescence spectra were acquired using a microplate reader (Tecan Infinite M200) or an Eppendorf biospectrometer kinetic device. All measurements were conducted at 25 °C. Extinction coefficient of fluorophore was determined by using 20 μM solutions in aqueous buffer and calculated based on the Lambert−Beer law.

Degree of Labeling. The degree of labeling (DOL) is defined as the average number of dye molecules coupled to CDs derivatives.[39] The DOL can be determined from the absorption spectrum of a marker against the corresponding free dye standard solution of known concentration.[45] The calibration curves were performed in a series of known concentrations of free dyes (Tables S4 and S6). Their corresponding UV absorption was measured and calibration curves were performed on the basis of the UV absorption values (Figures S3 and S4). Subsequently, absorbances of FITC−HPCDs, fluorescein−HPCDs, and XITC−HPCDs with corresponding concentration were measured, and their degree of labeling was calculated based on the calibration curves and eq 1.

$$\mathrm{DOL} = \frac{C1}{\mathrm{MW1}} \times \frac{(\mathrm{MW2} + \mathrm{MW1} \times \mathrm{DOL})}{C2} \quad (1)$$

where $C1$ is the concentration of the dye labeled in HPCDs, MW1 is the molecular weight of dye, MW2 is the average molecular weight of HPCD, $C2$ is the concentration of markers (dye conjugated with HPCD), and DOL is the value of degree of labeling.

Dynamic Light Scattering Analysis. Dynamic light scattering (DLS) studies were conducted on aqueous solutions of FITC−HPCDs and fluorescein−HPCDs. The samples were prepared at the desired concentration (3 mM) and filtered through a sterile 0.22 μm filter before analysis. The Zetasizer Nano S90 uses a 633 nm helium−neon laser. The measurements were carried out in quadratic cells, and the scattered light was analyzed at an angle of 90° at a controlled temperature (25 °C). All samples were analyzed in triplicate using the DTS Software from Malvern Instruments. The intensity of scattering of a particle is assumed to be proportional to the sixth power of its diameter. The apparent hydrodynamic radius was calculated according to the Stokes−Einstein equation.

Plasma Protein Binding. A marker-protein stock solution was prepared by incubating 2 mL of the corresponding marker (1 mg/mL in PBS) with 8 mL of Sprague−Dawley rat plasma in Li−heparin (Innovative Research, Novi, MI) at 37 °C, and 2 mL of PBS was incubated with 8 mL of rat plasma as control. Plasma protein binding measurements were performed by equilibrium dialysis of PBS against marker-protein stock solution (or control stock solution) using a two-chamber dialysis setup. After 24 h, the absorption of each of the markers in PBS and plasma were determined in three independent measurements by both absorption spectroscopy and fluorescence spectroscopy in a microplate reader. The concentrations of each of the markers were calculated on the basis of the corresponding molar absorption coefficients.[52−54] All experiments were performed in triplicate. PPB of each of the markers in percent [%] was determined by averaging three independent measurements and following the equation of the Lambert−Beer law: $\mathrm{PPB} = [A_{\mathrm{plasma}} - A_{\mathrm{PBS}}]/[A_{\mathrm{plasma}} + A_{\mathrm{PBS}}] \times 100\%$ (2), where A is corresponding to UV absorption.

Stability Studies in Esterase and Plasma. The mixtures of plasma or porcine liver esterase (PLE, 20 mg/mL, 150 unit/mL) with each of the markers (50 mg/mL in sodium phosphate buffer solution, pH 7.5−8.0) were incubated at 37 °C for 24 h. After incubation, they are filtered via sterile syringe filter with a membrane pore size of 0.22 μm and transferred to a proper vial. Samples of three control groups such as plasma, native fluorophore, and the corresponding marker were prepared according to the same procedure. Plasma and esterase enzymatic degradation were monitored by injecting 30 μL of each sample into HPLC. The gradient program A is described in Table S1.

Cytotoxicity Analysis. The cytotoxicity of FITC−HPβCD and fluorescein−HPCDs was evaluated by using standard (4,5-dimethyl-2-thiazolyl)-2,5-diphenyltetrazolium bromide (MTT) assay in a 96 well plate set up to assess the viability of cultured cells. A pair of conditionally immortalized human proximal tubule cell lines (ciPTEC),[58] which overexpress either the organic anion transporter ciPTEC-OAT1 or ciPTEC-OAT3, were used as in vitro models. Cells were cultured as follows: densities of 55 000 cells p/cm^2 for ciPTEC-OAT1 and 83 000 cells p/cm^2 for ciPTEC-OAT3 were used. Cells were grown at 33 °C for 24 h and matured for 7 days at 37 °C prior to all assays. Cells were incubated for 3 h at 37 °C with various concentrations of FITC−HPβCD and fluorescein−HPCDs (0.006, 0.013, 0.025, 0.05, 0.1, and 0.2 mg/mL) in Hank's balanced salt solution (HBSS, an isotonic solution used for washing and incubating cells; Gibco). After the treatment cells were washed two times with HBSS and incubated with 5 mg/mL MTT, they were freshly prepared in HBSS for 3 h. After MTT incubation, cells were washed two times with HBSS and 100 μL of dimethyl sulfoxide (DMSO) was added to the wells (to dissolve MTT crystals). The plates were then placed in an orbital shaker for a minimum of 30 min, and subsequently, absorbance was measured at 570 nm. The cell viability was calculated as the ratio of the absorbance of the sample to that of the control cells and expressed as a percentage. All experiments were performed in triplicate.

Principle and Method of Transcutaneous Measurement. The transcutaneous assessment of renal function is based on the measurement of the fluorescence signal of a marker through the skin. Briefly, a miniaturized transcutaneous device contains two light emitting diodes (LEDs) and one photodiode (Figure S1). The LEDs can blink every few seconds to excite a fluorescent marker using excitation wavelength at 480 nm. The fluorescent signal will be recorded by detecting the emission wavelength at 520 nm. Data are stored in the device and can be read out after measurement.[22,27] The clearance half-life of fluorescent markers was calculated by software, which was developed by the Institute of Medical Technology of the University of Heidelberg.[63] For this, a three-exponential function was fitted to the measured elimination curve; the peak of the curve was assumed to be 100%. A one-exponential function was also applied from 50% to 15% of the peak height.

Sprague−Dawley rats were anesthetized for a short period with Isoflurane (Forene, AbbVie, North Chicago, IL; dosage:

DOI: 10.1021/acs.bioconjchem.6b00452
Bioconjugate Chem. 2016, 27, 2513−2526

5%; flow (O_2): 5 L/min) so that a transcutaneous device could be attached to the back of rats and a fluorescent marker solution injected. The back of the animals was depilated with an electric shaver and depilation creme (Veet, Reckitt-Benckiser, Slough, U.K.) to avoid autofluorescence of the fur. After a baseline measurement was made for around 5 min, a fluorescent marker in saline (DeltaSelect, GmbH, Rimbach, Germany) was injected as a bolus by tail vein injection. The dosages of fluorescent markers are dependent on fluorescent quantum yield and degree of labeling of each marker (FITC−HPCDs: 50 mg/kg, fluorescein−HPCDs: 50 mg/kg, XITC−HPβCD: 180 mg/kg,). Rats were conscious during the measurement and housed in separate cages. The devices were removed and the data read out after 120 min of transcutaneous measurement. In probenecid inhibition studies, Sprague−Dawley rats were treated in the same manner as described above. The rats group received 50 mg/kg probenecid intraperitoneally injection 30 min prior to injection of the test markers. Conversion of clearance half-life into GFR can be performed if needed. The method is based on our previous studies.[26,28] All experiments were conducted in accordance with the German Animal Protection Law and approved by the local authority (Regierungspräsidium Nordbaden, Karlsruhe Germany in agreement with EU guideline 2010/63/EU).

Urinary Recovery of Injected Doses. Recovery of the injected dose in urine studies were conducted in conscious SD rats. The corresponding test markers with corresponding dosage (5 mg/100 g body weight) were administered by tail vein injection. Urine was collected using metabolic cages in intervals of 1, 2, 3, 6, 9, and 24 h after the intravenous injection of markers into rats. The urine samples were centrifuged for 8 min at 13000*g* and then filtered by 0.22 μm syringe filter. A series of working solution of each marker with concentrations between 0.02 and 2 mg/mL were prepared. Appropriate volumes of the working solutions were added to blank urine, and fluorescent intensity of those mixtures were measured to obtain an external calibration curve. Quantification of each of the markers in urine at each time point was performed via HPLC analysis and fluorescence intensity detection. The concentration in urine at each time point was calculated based on the external calibration standards curve between fluorescence intensity and the concentration of each of the markers. The samples handling and measuring procedures were similar to that described for plasma protein binding and labeling degree measurement.

Determination of Urinary Metabolites. Urine samples were collected and stored at −20 °C until analysis. Urine samples were centrifuged for 8 min at 13000*g* and then filtered by 0.22 μm syringe filter. The filtered urine samples were determined by HPLC. The gradient program B is described in Table S1. Select portions of the eluent were collected on the basis of the processed signal and measured by a mass spectrometer.

■ ASSOCIATED CONTENT

Supporting Information

The Supporting Information is available free of charge on the ACS Publications website at DOI: 10.1021/acs.bioconjchem.6b00452.

Tables showing gradient program A, commonly used exogenous and endogenous markers for GFR measurements in humans, physicochemical properties of the natural CDs and 2-hydroxylpropyl-CDs, absorbance of FITC and fluorescein, absorption and degree of labeling of FITC−HPCDs and fluorescein−HPCDs, absorbance of XITC, absorption and degree of labeling of XITC−HPCDs, results of DLS measurements, results of the assessment of protein plasma binding, and urinary recovery values. Figures showing transcutaneous device and battery used for the transcutaneous measurement, a schematic overview of the excitation and emission light between a transcutaneous device and fluorescent markers in capillary vessel after injection, absorption and emission spectra of each of the markers in rat plasma supplemented with 1× PBS at 25 °C, linear calibration curve of FITC and fluorescein, linear calibration curve of XITC, DLS data, HPLC chromatographs, cell viability of ciPTEC-OAT1 and ciPTEC-OAT3 cells incubated with FITC−HPβCD, fluorescein−HPCDs by MTT assays, transcutaneous measured elimination curves, Bland−Altman plots from the transcutaneous measurement without and with probenecid treatment, urinary recovery values, evaluation of each marker from recovered urine samples using HPLC assay (gradient program B) and mass spectrometry, and NMR results and mass spectrometry of compounds. Additional details on the degree of labeling and stability studies. (PDF)

■ AUTHOR INFORMATION

Corresponding Author

*E-mail: Norbert.Gretz@medma.uni-heidelberg.de.

Author Contributions

⊥These authors contributed equally to this work.

Notes

The authors declare no competing financial interest.

■ ACKNOWLEDGMENTS

This work was supported by the FP7Marie Curie ITN project: Nephrotools. J.H. is a Marie Curie Fellow within the Nephrotools Project. We thank Prof. Björn Wängler and Dr. Carmen Wängler for assistance in providing chemicals for the lab. We further thank Dr. Uwe Seibold and Dr. Hermelindis Ruh for technical assistance with mass spectra experiments. We also thank Victoria Skude and Elisabeth Wühl for their technical assistance with the animal experiments.

■ REFERENCES

(1) Stevens, L. A., and Levey, A. S. (2009) Measured GFR as a confirmatory test for estimated GFR. *J. Am. Soc. Nephrol. 20*, 2305−2313.

(2) Radford, R., Frain, H., Ryan, M. P., Slattery, C., and McMorrow, T. (2013) Mechanisms of chemical carcinogenesis in the kidneys. *Int. J. Mol. Sci. 14*, 19416−19433.

(3) Abbink, F. C., Laarman, C. A., Braam, K. I., van Wijk, J. A., Kors, W. A., Bouman, A. A., Spreeuwenberg, M. D., Stoffel-Wagner, B., and Bökenkamp, A. (2008) Beta-trace protein is not superior to cystatin C for the estimation of GFR in patients receiving corticosteroids. *Clin. Biochem. 41*, 299−305.

(4) Herget-Rosenthal, S., Bokenkamp, A., and Hofmann, W. (2007) How to estimate GFR-serum creatinine, serum cystatin C or equations? *Clin. Biochem. 40*, 153−161.

(5) Schwartz, G. J., and Furth, S. L. (2007) Glomerular filtration rate measurement and estimation in chronic kidney disease. *Pediatr. Nephrol. 22*, 1839−1848.

DOI: 10.1021/acs.bioconjchem.6b00452
Bioconjugate Chem. 2016, 27, 2513−2526

(6) Stevens, L. A., Coresh, J., Greene, T., and Levey, A. S. (2006) Assessing kidney function - measured and estimated glomerular filtration rate. *N. Engl. J. Med. 354*, 2473−2483.
(7) Bokenkamp, A., Herget-Rosenthal, S., and Bokenkamp, R. (2006) Cystatin C, kidney function and cardiovascular disease. *Pediatr. Nephrol. 21*, 1223−1230.
(8) Filler, G., Bokenkamp, A., Hofmann, W., Le Bricon, T., Martinez-Bru, C., and Grubb, A. (2005) Cystatin C as a marker of GFR–history, indications, and future research. *Clin. Biochem. 38*, 1−8.
(9) Diskin, C. J. (2006) Creatinine and GFR: an imperfect marriage of convenience. *Nephrol., Dial., Transplant. 21*, 3338−3339.
(10) Levey, A. S. (1990) Measurement of renal function in chronic renal disease. *Kidney Int. 38*, 167−184.
(11) Vilhelmsdotter Allander, S., Marke, L. A., Wihlen, B., Svensson, M., Elinder, C. G., and Larsson, A. (2012) Regional variation in use of exogenous and endogenous glomerular filtration rate (GFR) markers in Sweden. *Upsala J. Med. Sci. 117*, 273−278.
(12) Russell, C. D. (1993) Optimum sample times for single-injection, multisample renal clearance methods. *J. Nucl. Med. 34*, 1761−1765.
(13) Chinen, L. K., Galen, K. P., Kuan, K. T., Dyszlewski, M. E., Ozaki, H., Sawai, H., Pandurangi, R. S., Jacobs, F. G., Dorshow, R. B., and Rajagopalan, R. (2008) Fluorescence-enhanced europium-ei-ethylene triamine pentaacetic (DTPA)- monoamide complexes for the assessment of renal function. *J. Med. Chem. 51*, 957−962.
(14) Rajagopalan, R., Neumann, W. L., Poreddy, A. R., Fitch, R. M., Freskos, J. N., Asmelash, B., Gaston, K. R., Shieh, J. J., Dorshow, R. B., and Galen, K. P. (2011) Hydrophilic pyrazine dyes as exogenous fluorescent tracer agents for real-time point-of-care measurement of glomerular filtration rate. *J. Med. Chem. 54*, 5048−5058.
(15) Poreddy, A. R., Neumann, W. L., Freskos, J. N., Rajagopalan, R., Asmelash, B., Gaston, K. R., Fitch, R. M., Shieh, J. J., Dorshow, R. B., and Galen, K. P. (2012) Exogenous fluorescent tracer agents based on pegylated pyrazine dyes for real-time point-of-care measurement of glomerular filtration rate. *Bioorg. Med. Chem. 20*, 2490−2497.
(16) Bugaj, J. E., and Dorshow, R. B. (2015) Pre-clinical toxicity evaluation of MB-102, a novel fluorescent tracer agent for real-time measurement of glomerular filtration rate. *Regul. Toxicol. Pharmacol. 72*, 26−38.
(17) Lorenz, J. N., and Gruenstein, E. (1999) A simple, non-radioactive method for evaluating single-nephron filtration rate using FITC-inulin. *Am. J. Physiol. 276*, F172−177.
(18) Qi, Z., Whitt, I., Mehta, A., Jin, J., Zhao, M., Harris, R. C., Fogo, A. B., and Breyer, M. D. (2004) Serial determination of glomerular filtration rate in conscious mice using FITC-inulin clearance. *Am. J. Physiol. Renal. Physiol. 286*, 590F−596.
(19) Pill, J., Issaeva, O., Woderer, S., Sadick, M., Kranzlin, B., Fiedler, F., Klötzer, H. M., Krämer, U., and Gretz, N. (2006) Pharmacological profile and toxicity of fluorescein-labelled sinistrin, a novel marker for GFR measurements. *Naunyn-Schmiedeberg's Arch. Pharmacol. 373*, 204−211.
(20) Pill, J., Kraenzlin, B., Jander, J., Sattelkau, T., Sadick, M., Kloetzer, H. M., Deus, C., Kraemer, U., and Gretz, N. (2005) Fluorescein-labeled sinistrin as marker of glomerular filtration rate. *Eur. J. Med. Chem. 40*, 1056−1061.
(21) Pill, J., Kloetzer, H. M., Issaeva, O., Kraenzlin, B., Deus, C., Kraemer, U., Sadick, M., Fiedler, F., and Gretz, N. (2005) Direct fluorometric analysis of a newly synthesised fluorescein-labelled marker for glomerular filtration rate. *Anal. Bioanal. Chem. 382*, 59−64.
(22) Schock-Kusch, D., Xie, Q., Shulhevich, Y., Hesser, J., Stsepankou, D., Sadick, M., Koenig, S., Hoecklin, F., Pill, J., et al. (2011) Transcutaneous assessment of renal function in conscious rats with a device for measuring FITC-sinistrin disappearance curves. *Kidney Int. 79*, 1254−1258.
(23) Steinbach, S., Krolop, N., Strommer, S., Herrera-Perez, Z., Geraci, S., Friedemann, J., Gretz, N., and Neiger, R. (2014) A pilot study to assess the feasibility of transcutaneous glomerular filtration rate measurement using fluorescence-labelled sinistrin in dogs and cats. *PLoS One 9*, e111734−111743.
(24) Huang, J., Gretz, N., and Weinfurter, S. (2016) Filtration markers and determination methods for the assessment of kidney function. *Eur. J. Pharmacol.* 10.1016/j.ejphar.2016.06.060.
(25) Cowley, A. W., Ryan, R. P., Kurth, T., Skelton, M. M., Schock-Kusch, D., and Gretz, N. (2013) Progression of glomerular filtration rate reduction determined in conscious Dahl salt-sensitive hypertensive rats. *Hypertension 62*, 85−90.
(26) Schreiber, A., Shulhevich, Y., Geraci, S., Hesser, J., Stsepankou, D., Neudecker, S., Koenig, S., Heinrich, R., Hoecklin, F., Pill, J., et al. (2012) Transcutaneous measurement of renal function in conscious mice. *Am. J. Physiol. Renal. Physiol. 303*, F783−788.
(27) Schock-Kusch, D., Shulhevich, Y., Xie, Q., Hesser, J., Stsepankou, D., Neudecker, S., Koenig, S., Heinrich, R., Hoecklin, F., Pill, J., et al. (2012) Online feedback-controlled renal constant infusion clearances in rats. *Kidney Int. 82*, 314−320.
(28) Schock-Kusch, D., Sadick, M., Henninger, N., Kraenzlin, B., Claus, G., Kloetzer, H. M., Weiss, C., Pill, J., and Gretz, N. (2009) Transcutaneous measurement of glomerular filtration rate using FITC-sinistrin in rats. *Nephrol., Dial., Transplant. 24*, 2997−3001.
(29) Kolodziejczyk, R., Michalska, K., Hernandez-Santoyo, A., Wahlbom, M., Grubb, A., and Jaskolski, M. (2010) Crystal structure of human cystatin C stabilized against amyloid formation. *FEBS J. 277*, 1726−1737.
(30) Loftsson, T., and Brewster, M. E. (2010) Pharmaceutical applications of cyclodextrins: basic science and product development. *J. Pharm. Pharmacol. 62* (11), 1607−1621.
(31) Lumholdt, L. R., Holm, R., Jorgensen, E. B., and Larsen, K. L. (2012) In vitro investigations of α-amylase mediated hydrolysis of cyclodextrins in the presence of ibuprofen, flurbiprofen, or benzo[a]-pyrene. *Carbohydr. Res. 362*, 56−61.
(32) Sato, S., Umeda, Y., Fujii, S., and Takenaka, S. (2015) Cooperative binding of ferrocenylnaphthalene diimide carrying β-cyclodextrin converts double-stranded DNA to a rod-like structure. *Bioconjugate Chem. 26*, 379−382.
(33) Takechi-Haraya, Y., Tanaka, K., Tsuji, K., Asami, Y., Izawa, H., Shigenaga, A., Otaka, A., Saito, H., and Kawakami, K. (2015) Molecular complex composed of β-cyclodextrin-grafted chitosan and pH-sensitive amphipathic peptide for enhancing cellular cholesterol efflux under acidic pH. *Bioconjugate Chem. 26*, 572−581.
(34) Liu, J., Hennink, W. E., Van Steenbergen, M. J., Zhuo, R., and Jiang, X. (2016) Versatile supramolecular gene vector based on host-guest interaction. *Bioconjugate Chem. 27*, 1143−1152.
(35) Malanga, M., Szemán, J., Fenyvesi, É., Puskás, I., Csabai, K., Gyémánt, G., Fenyvesi, F., and Szente, L. (2016) Back to the future: a new look at hydroxypropyl beta-cyclodextrins. *J. Pharm. Sci. 105* (9), 2921−2931.
(36) Fujikawa, Y., Urano, Y., Komatsu, T., Hanaoka, K., Kojima, H., Terai, T., Inoue, H., and Nagano, T. (2008) Design and synthesis of highly sensitive fluorogenic substrates for glutathione S-transferase and application for activity imaging in living cells. *J. Am. Chem. Soc. 130*, 14533−14543.
(37) Yang, Y., Escobedo, J. O., Wong, A., Schowalter, C. M., Touchy, M. C., Jiao, L., Crowe, W., Fronczek, R., and Strongin, R. M. (2005) A convenient preparation of xanthene dyes. *J. Org. Chem. 70*, 6907−6912.
(38) Shi, J., Zhang, X., and Neckers, D. C. (1992) Xanthenes: fluorone derivatives. *J. Org. Chem. 57*, 4418−4421.
(39) Urano, Y., Kamiya, M., Kanda, K., Ueno, T., Hirose, K., and Nagano, T. (2005) Evolution of fluorescein as a platform for finely tunable fluorescence probes. *J. Am. Chem. Soc. 127*, 4888−4894.
(40) Fenyvesi, F., Réti-Nagy, K., Bacsó, Z., Gutay-Tóth, Z., Malanga, M., Fenyvesi, É., Szente, L., Váradi, J., Ujhelyi, Z., Fehér, P., Szabó, G., et al. (2014) Fluorescently labeled methyl-beta-cyclodextrin enters intestinal epithelial Caco-2 cells by fluid-phase endocytosis. *PLoS One 9* (1), e84856.
(41) Malanga, M., Darcsi, A., Balint, M., Benkovics, G., Sohajda, T., and Beni, S. (2016) New synthetic strategies for xanthene-dye-appended cyclodextrins. *Beilstein J. Org. Chem. 12*, 537−548.

DOI: 10.1021/acs.bioconjchem.6b00452
Bioconjugate Chem. 2016, 27, 2513−2526

(42) Malanga, M., Bálint, M., Puskás, I., Tuza, K., Sohajda, T., Jicsinszky, L., Szente, L., and Fenyvesi, É. (2014) Synthetic strategies for the fluorescent labeling of epichlorohydrin-branched cyclodextrin polymers. *Beilstein J. Org. Chem. 10*, 3007−3018.
(43) Marius, P., Leung, Y. M., Piggot, T. J., Khalid, S., and Williamson, P. T. (2012) Probing the oligomeric state and interaction surfaces of Fukutin-I in dilauroylphosphatidylcholine bilayers. *Eur. Biophys. J. 41*, 199−207.
(44) Lee, J. H., Schneider, B., Jordan, E. K., Liu, W., and Frank, J. A. (2008) Synthesis of complexable fluorescent superparamagnetic iron oxide nanoparticles (FL SPIONs) and cell labeling for clinical application. *Adv. Mater. 20*, 2512−2516.
(45) Vira, S., Mekhedov, E., Humphrey, G., and Blank, P. S. (2010) Fluorescent-labeled antibodies: balancing functionality and degree of labeling. *Anal. Biochem. 402*, 146−150.
(46) Longmire, M., Choyke, L., and Kobayashi, H. (2008) Clearance properties of nano-sized particles and molecules as imaging agents: considerations and caveats. *Nanomedicine 3*, 703−717.
(47) Herbois, R., Noel, S., Leger, B., Bai, L., Roucoux, A., Monflier, E., and Ponchel, A. (2012) Cyclodextrins as growth controlling agents for enhancing the catalytic activity of PVP-stabilized Ru(0) nanoparticles. *Chem. Commun. 48*, 3451−3453.
(48) Bonini, M., Rossi, S., Karlsson, G., Almgren, M., Lo Nostro, P., and Baglioni, P. (2006) Self-assembly of β-cyclodextrin in water. part 1: cryo-TEM and dynamic and static light scattering. *Langmuir 22*, 1478−1484.
(49) Li, H., Meng, B., Chai, S., Liu, H., and Dai, S. (2016) Hypercrosslinked β-cyclodextrin porous polymer: an adsorption-facilitated molecular catalyst support for transformation of water-soluble aromatic molecules. *Chem. Sci. 7*, 905−909.
(50) Puskas, I., Schrott, M., Malanga, M., and Szente, L. (2013) Characterization and control of the aggregation behavior of cyclodextrins. *J. Inclusion Phenom. Mol. Recognit. Chem. 75*, 269−276.
(51) Gleeson, M. P. (2007) Plasma protein binding affinity and its relationship to molecular structure: an in-silico analysis. *J. Med. Chem. 50*, 101−112.
(52) Scarfe, L., Rak-Raszewska, A., Geraci, S., Darssan, D., Sharkey, J., Huang, J., Burton, N. C., Mason, D., Ranjzad, P., Kenny, S., et al. (2015) Measures of kidney function by minimally invasive techniques correlate with histological glomerular damage in SCID mice with adriamycin-induced nephropathy. *Sci. Rep. 5*, 13601−13614.
(53) Licha, K., Riefke, B., Ntziachristos, V., Becker, A., Chance, B., and Semmler, W. (2000) Hydrophilic cyanine dyes as contrast agents for near-infrared tumor imaging: synthesis, photophysical properties and spectroscopic in vivo characterization. *Photochem. Photobiol. 72*, 392−398.
(54) Hamann, F. M., Brehm, R., Pauli, J., Grabolle, M., Frank, W., Kaiser, W. A., Fischer, D., Resch-Genger, U., and Hilger, I. (2011) Controlled modulation of serum protein binding and biodistribution of asymmetric cyanine dyes by variation of the number of sulfonate groups. *Mol. Imaging. 10*, 258−269.
(55) Rockey, J. H., Li, W., and Eccleston, J. F. (1983) Binding of fluorescein and carboxyfluorescein by human serum proteins: significance of kinetic and equilibrium parameters of association in ocular fluorometric studies. *Exp. Eye Res. 37*, 455−466.
(56) Smith, D. A., Di, L., and Kerns, E. H. (2010) The effect of plasma protein binding on in vivo efficacy: misconceptions in drug discovery. *Nat. Rev. Drug Discovery 9*, 929−939.
(57) Tamm, C. (1992) Pig liver esterase catalyzed hydrolysis: substrate specificity and stereoselectivity. *Pure Appl. Chem. 64* (8), 1187−1191.
(58) Nieskens, T. T., Peters, J. G., Schreurs, M. J., Smits, N., Woestenenk, R., Jansen, K., Van der Made, T. K., Röring, M., Hilgendorf, C., Wilmer, M. J., et al. (2016) A human renal proximal tubule cell line with stable organic anion transporter 1 and 3 expression predictive for antiviral-induced toxicity. *AAPS J. 18*, 465−475.
(59) Kiss, T., Fenyvesi, F., Bácskay, I., Váradi, J., Fenyvesi, E., Iványi, R., Szente, L., Tósaki, A., and Vecsernyés, M. (2010) Evaluation of the cytotoxicity of beta-cyclodextrin derivatives: evidence for the role of cholesterol extraction. *Eur. J. Pharm. Sci. 40* (4), 376−380.
(60) Mustafa, D., Ma, D., Zhou, W., Meisenheimer, P., and Cali, J. J. (2016) Novel no-wash luminogenic probes for the detection of transporter uptake activity. *Bioconjugate Chem. 27*, 87−101.
(61) Izumi, S., Nozaki, Y., Komori, T., Takenaka, O., Maeda, K., Kusuhara, H., and Sugiyama, Y. (2016) Investigation of fluorescein derivatives as substrates of organic anion transporting polypeptide (OATP) 1B1 to develop sensitive fluorescence-based OATP1B1 inhibition assays. *Mol. Pharmaceutics 13*, 438−448.
(62) Blair, N. P., Evans, M. A., Lesar, T. S., and Zeimer, R. C. (1986) Fluorescein and fluorescein glucuronide in the vitreous body of diabetic patients. *Invest. Ophthalmol. Vis. Sci. 27*, 1107−1114.
(63) Shmarlouski, A., Shulhevich, Y., Geraci, S., Friedemann, J., Gretz, N., Neudecker, S., Hesser, J., and Stsepankou, D. (2014) Automatic artifact removal from GFR measurements. *Biomed. Signal. Process. Control. 14*, 30−41.

DOI: 10.1021/acs.bioconjchem.6b00452
Bioconjugate Chem. 2016, 27, 2513−2526